

An improved BP Neural Network for Wastewater Bacteria Recognition Based on Microscopic Image Analysis

LI XIAOJUAN¹ CHEN CUNSHE²

¹College of Information Engineering Capital Normal University Beijing 100037, China

²school of Chemical and Environmental Engineering, Beijing Technology and Business University
Beijing 100037, China
lixjxxxxy@263.net

Abstract: The microscopic images of wastewater bacteria are analysed, and a scheme for classification and recognition for wastewater bacteria based on microscopic images analysis are put forward in the paper. An adaptive and enhanced edge detection solution for the images of wastewater bacteria is proposed, which can effectively remove noises in the images and get clear edges of microscopic image by optimizing segmentation threshold and the varied order of edge detection. Seven contour invariant moment features and four morphological features are extracted by analysis of microscopic images of wastewater bacteria in which six features are chosen by PCA in order to reduce the dimensionality of the features extracted from the images. A self-adaptive accelerated BP algorithm is developed for training the classification of bacteria microscopic images. The proposed method is tested with CECC database and the results show that the presented image recognition solution is effective and can greatly improve the speed and consistency in performing large-scale surveys or rapid determination of bacterial abundance, morphology.

Keywords: BP Neural Network, Edge Detection, Wastewater Bacteria, Contour Invariant moment.

1 Introduction

Filtered fluorescently dyed cells is the typically way for the determination of wastewater bacterial abundance, biovolume and morphology microscopic examination. Identification, counting and measuring individual cells based on examining are normally done manually, which is tedious and time-consuming. However, image analysis is a efficient way to do that automatically. In the paper a novel image of bacteria recognition scheme is presented, which can be used for versatile, efficient processing of many images in order to obtain reliable, high-resolution data of microorganisms. An adaptive and enhanced edge detection solution for the images of wastewater bacteria is proposed which is effective for the edge detection of bacteria images by optimizing threshold value for segmentation combining with mathematical morphology method, which effectively remove or restrain noise and get clear edges of microscopic image (Massana R et al., 1997). Principal component analysis is used to reduce the dimensionality of original features extracted from the images and a improved BP network is introduced to train for the bacteria images recognition. A effective bacteria image recognition can greatly improve the speed and consistency in performing large-scale surveys or rapid determination of bacterial abundance, morphology

and makes sampling at a higher resolution than is practical manually.

2 Edge Detection and contour definition for the Image of Wastewater Bacteria

The edge of an image is one of the fundamental features for digital images, which is the basis of image segmentation, features extraction and recognition for aim area. The edges of objects become blurred when they are viewed at high magnification, which is caused by the limited resolution of microscope optics. Moreover, uneven lighting and differences in exposure times and object luminescence make it impossible to choose a single gray level as a threshold for distinguishing objects from the background. Viles and Sieracki (Sieracki, M. E. et al. 1992) discussed this problem with respect to bacteria under epifluorescence conditions and concluded that a Marr-Hildreth operator functions with a high degree of independence for exposure and lighting characteristics and with accurate edge detection properties. A Marr-Hildreth operator is a combination of a Gaussian operator for smoothing and a Laplace operator for amplifying high spatial frequencies. The Laplace operator calculates the second derivative of intensity. If the edge of a

blurred object is at the point where the rate of intensity change is greatest (second derivative), the Laplace operator identifies its position as the zero crossing between positive and negative values. However, the Laplace operator is sensitive to electronic camera noise and to faint particles, which can be a problem for analysis of the images with noisy signals. So we propose a method of edge detection for bacteria images, which is combined the iterative threshold value segmentation with mathematical morphology edge detection.

2.1 Algorithm for Adaptive threshold value determination

The segment of a object image with threshold is to find the edge of the object image in the background, in which the gray level is different, by setting the proper gray level threshold. Theoretically, assume that g is a proper segmenting threshold, g can be used to detect to the edge of the object from the background; furthermore, the gray histogram of the image will show two obvious submits if the image of a object is universally distributed on the background. But in practice it is difficult to locate the correct point of the peak and vale due to the noise in images. So we develop a method of adaptive threshold value determination to erase the effect of noises on threshold value(g) determination. A image with a noises can be denoted by:

$$g(x, y) = f(x, y) + e(x, y) \tag{1}$$

in which the $f(x,y)$ is a image information, and $e(x,y)$ is noises. By threshold segmentaion a image can be divided into two parts as following:

$$g_1(x, y) = f_1(x, y) + e(x, y) \tag{2}$$

$$g_2(x, y) = f_2(x, y) + e(x, y) \tag{3}$$

Since the noises in images are assumed random the noises $e(x,y)$ still exit both in object image part and background part, and the gray level mean value is computed with iterative threshold :

$$E\{g_1(x, y)\} = E\{f_1(x, y) + e(x, y)\} = E\{f_1(x, y)\} \tag{4}$$

$$E\{g_2(x, y)\} = E\{f_2(x, y) + e(x, y)\} = E\{f_2(x, y)\}$$

(5)

The above formula denote that gray level mean value is getting close to true value with increasing of iteration. So the optimized

threshold can be attained in which noises information is excluded.

The iterative improved policy on threshold value is the key factor of the algorithm(Li Xiaojuan et al., 2007). Initially a approximation threshold value is selected, by which a image is segmented and produces sub-images, and then a new threshold value is selected dependent on the features of the sub-images. The new threshold value is continues used to segment the images and so on, until the error pixel of the images is minimized:

1. Initially a estimated threshold value is determined:

$$T^0 = \{T^k \mid k = 0\} \tag{6}$$

$$T_0 = \frac{Z_{min} + Z_{max}}{2}$$

Z_{min} Z_{max} is respectively the minimum and maximum gray level of the image

2. The Image is divided into two areas(R1 and R2) by T^k

$$R1 = \{f(x, y) \mid f(x, y) \geq T^k\} \tag{7}$$

$$R2 = \{f(x, y) \mid 0 < f(x, y) < T^k\}$$

3. Figure out the median of gray level of area R1 and area R2

$$Z_1 = \frac{\sum_{f(i,j) < T^k} f(i, j) \times N(i, j)}{\sum_{f(i,j) < T^k} N(i, j)} \tag{8}$$

$$Z_2 = \frac{\sum_{f(i,j) > T^k} f(i, j) \times N(i, j)}{\sum_{f(i,j) > T^k} N(i, j)} \tag{9}$$

$f(i,j)$ is the gray level at pixel (i,j) $N(i,j)$ is weigh factor.

4. A new threshold value T^{k+1} is determined

$$T^{k+1} = \frac{Z_1 + Z_2}{2} \tag{10}$$

If $k=T^{k+1}$, the segmentation is completed else $k=K+1$, continue to step to (2) above. Edge detection for identification of objects was performed with the optimal threshold value, which produced a binary image. Most of the background noise was effectively removed.

2.2 Enhanced Edge Detection

The process of threshold value segmentation

remove or restrain most of the background noise by the optimal threshold value, but it might be falsely associated with the edges of objects, and result in the blurred edge of image. Mathematics morphologic methods is a useful for pre-processing or image analysis based on the flat structuring element operation. the structuring element operator is vital to the result of image process. In the paper the erosion operation in mathematical morphology is used to improve the edge clarity of images, and erosion operation is performed on the binary image with 5x5 structure element, by which image edges with only one- pixel width is attained and results in the binary image used for measurement and recognition, as shown in figure 4.

Analysis and a series of tests(CECC database) show that the edge detection of bacteria microscopic image based on iterative threshold value segmentation and mathematical morphology can not only effectively remove or restrain noise but also get clear edges of microscopic image by determining proper threshold value for segmentation and changing the order of edge detection. Fig.1 shows a original microscopic image of bacteria, Fig. 2 is the result of edge detection with Sobel operator in which the noise is blended among edge pixel and might result in unstable edge. Fig. 3 is the result of edge detection with Gauss-Laplace, some of edge information about aim object is lost and made the edge is noncontiguous or isolated for that Laplace operator is sensitive to electronic camera noise and to faint particles.



Fig. 1 the original image

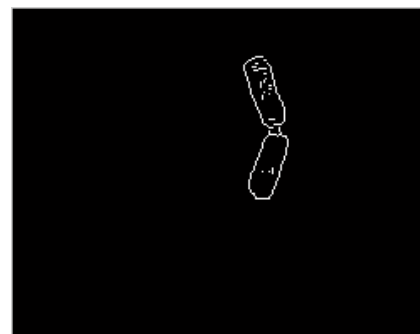


Fig.2 edge detection with Sobel operator

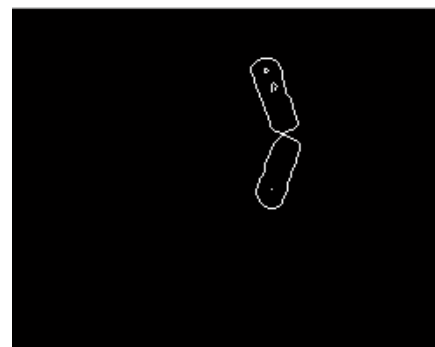


Fig.3 Gauss-Laplace edge detection

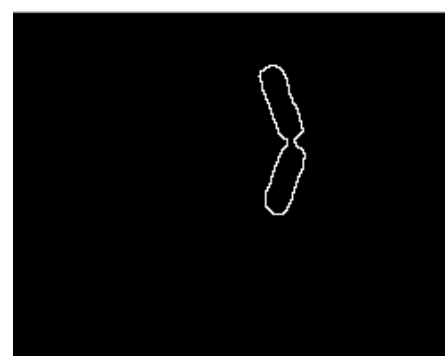


Fig. 4 edge detection with adaptive enhanced edge detection

Edge detection we proposed for bacteria identification intensify the aim object of microscopic image and enhance the clarity of edges by iterating for proper threshold value while exactly locate the aim objects and segment it from background that achieved by combining the iterative threshold value segmentation theory with mathematical morphology edge detection. The method of edge detection is noise-proof robust, and can be well balanced between refraining noise and the retained whole fine edges of aim objects.

3 Extraction Features of Microscopic Image

The primitive features which effectively describe the information of aim bacteria have to be abstracted from the object image after segmentation. There are many kinds of features for construction or recognition a objects by their image, such as geometry features, algebra features, texture features and transformation space features etc. Research on a amount of bacteria images shows that there is great difference in shape , morphology feature, even in texture feature for some bacteria, among different bacteria. As a result of images analysis for different kinds bacteria in wastewater, contour Invariant moment features and morphological features are used to describe the images of wastewater bacteria for their classification.

3.1 Contour Invariant moment features extraction

Moment is one of a broadly used shape features which is strongly related to the area, center, longest /breadth axel, of two-dimension image.Images recognition by the computer system can be based on some fecture values which are independent of the image scaling, translation and rotation and the values are called moment invariant (S.O. Belkasim, 1991,M. Shridha, et al,1991, C. Chen,1993). This method was firstly brought forward by M.K.Hu in 1962. He gave the definition and the property of continuous function momnet invariant. Moreover he proved the scaling, translation and rotation invariances and gave seven moment invariant functions for continuous function. Obviously the moment invariant functions by Hu need computing all pixels in target area. Though much arithmetic was researched by some researchers, they was fairly time-consuming(J. Flusser,2000, R.Mukundan,et al, 1995, G.L. Cash,1987). Target contour's pixels are generally much fewer than target area pixels, so the contour moment invariant which only need computing the moment of contour is put forward and its invariance for scaling, translation and rotation are further proved. The arithmetic has much advantage and it is called arithmetic contour moment invariant in order to distinguish Hu's moment invariant (J. Liu and T. Zhang.,2004, Y. Xu, 2002, S.O. Belkasim and M.Kamel,2001). The contour moment invariant is presented for continuous function's moment invariant; it means that it has the scale, translation and rotating invariances for continuous function. But mostly images to be recognized are described in discrete function in computers. If the arithmetic

contour moment invariant is used for discrete function, it only has the translation and rotating invariances and the scale invariances can not be kept. For this case, a improved contour moment invariant is provided in this paper. It keeps the scaling, translation and rotation invariances.

Invariant moment is statistic features of a image, and it is independent of changes of shift, enlarge or minimize and rotation which is useful for microbial image analysis and recognition. Hu (Hu .M.K., 1962) proposed invariant moment for recognition of definite area in an image as following:

For continuous function $f(x, y)$, the (p+q)th order geometric moment m_{pq} and it's central moment μ_{pq} is respectively defined as follow

$$m_{pq} = \int_{-\infty}^{+\infty} \int_{-\infty}^{+\infty} x^p y^q f(x, y) dx dy \quad (11)$$

$$\mu_{pq} = \int_{-\infty}^{+\infty} \int_{-\infty}^{+\infty} (x - \bar{x})^p (y - \bar{y})^q f(x, y) dx dy \quad (12)$$

$$p, q = 0, 1, 2, \dots$$

there, a image function could be a set of transformation coefficient m_{pq} , which is the projection of image into a group of 2-dimension multinomial primary function. Furthermore, for a $M \times N$ discrete digital image, the (p+q)th order geometric moment m_{pq} and it's central moment μ_{pq} respectively is,

$$m_{pq} = \sum_{x=1}^M \sum_{y=1}^N x^p y^q f(x, y) \quad (13)$$

$$\mu_{pq} = \sum_{x=1}^M \sum_{y=1}^N (x - \bar{x})^p (y - \bar{y})^q f(x, u) \quad (14)$$

$$p, q = 0, 1, 2, \dots$$

$$\text{here } \bar{x} = m_{10} / m_{00} \square \bar{y} = m_{01} / m_{00}$$

obviously $m_{00} = \mu_{00} \square \mu_{00}$ denotes quality of image for gray level image $\square \mu_{00}$ equal to the object area in a image for binary image. So normalized central moment can be as following:

$$\eta_{pq} = \mu_{pq} / \mu_{00}^r \quad r = 1 + p + q, \quad p + q = 2, 3, \dots \quad (15)$$

Hu constructs 7 invariant moments, which are independent of changes of shift, measurement and rotation by applying

algebra invariable theory to normalized second order and three order central moment:

$$\begin{aligned}
 \Phi_1 &= \eta_{20} + \eta_{02} \\
 \Phi_2 &= (\eta_{20} - \eta_{02})^2 + 4\eta_{11}^2 \\
 \Phi_3 &= (\eta_{30} - 3\eta_{12})^2 + (\eta_{03} + 3\eta_{21})^2 \\
 \Phi_4 &= (\eta_{30} + \eta_{12})^2 + (\eta_{03} + \eta_{21})^2 \\
 \Phi_5 &= (\eta_{30} - 3\eta_{12})(\eta_{30} - \eta_{12})[(\eta_{30} + \eta_{12})^2 - 3(\eta_{03} + \eta_{21})^2] \\
 &\quad + (3\eta_{21} - \eta_{03})(\eta_{21} + \eta_{03})[3(\eta_{30} + \eta_{12})^2 - (\eta_{03} + \eta_{21})^2] \\
 \Phi_6 &= (\eta_{20} - \eta_{02})[(\eta_{30} + \eta_{12})^2 - (\eta_{03} + \eta_{21})^2] + 4\eta_{11}(\eta_{30} + \eta_{12})(\eta_{03} + \eta_{21}) \\
 \Phi_7 &= (3\eta_{21} - \eta_{03})(\eta_{30} + \eta_{12})[(\eta_{30} + \eta_{12})^2 - 3(\eta_{03} + \eta_{21})^2] \\
 &\quad + (3\eta_{12} - \eta_{30})(\eta_{21} + \eta_{03})[3(\eta_{30} + \eta_{12})^2 - (\eta_{03} + \eta_{21})^2]
 \end{aligned} \tag{1}$$

The invariant moments above can be used in the field of image pattern, however, the invariant moments are based on field and closely relative to gray value of image, which might cause large computation. It is known that microbe is usually recognized according to its morphological feature in image, such as sphere, rod and crescent-shaped vibrios. In practice, the recognition process is based on the shape of cell in the image instead of its gray level, so we can simplify the invariant moments by computing contour moment based on the edge of microbe instead of the field. So we have to make sure whether the moments still keep the scaling, translation and rotation invariances if we use formula(15) for discrete data.

1. the translation invariances of moment feature

Let Δx stands for the translation quantity in x direction, Δy means the translation quantity in y direction and the formula is following:

$$\begin{cases} x' = x + \Delta x & (x, y) \in c \\ y' = y + \Delta y & (x', y') \in c' \end{cases} \tag{17}$$

(x, y) is the coordinate before translation and (x', y') is the coordinate after translation. From formula(13), we can obtain

$$m'_{pq} = \sum_{(x', y' \in c')} (x')^p (y')^q f'(x', y') \tag{18}$$

The relationship between $f'(x', y')$ and $f(x, y)$ should be as following:

$$f'(x', y') = f(x, y) \tag{19}$$

According to formula (14), we can obtain the following equation:

$$\begin{aligned}
 \mu'_{pq} &= \sum_{(x', y' \in c')} (x' - \bar{x}')^p (y' - \bar{y}')^q f'(x', y') \\
 &= \sum_{(x, y \in c)} (x + \Delta x - \frac{m'_{10}}{m'_{00}})^p (y + \Delta y - \frac{m'_{01}}{m'_{00}})^q f(x, y)
 \end{aligned}$$

$$\begin{aligned}
 &= \sum_{(x, y \in c)} \left\{ \left[\frac{\sum_{(x', y' \in c')} x' f'(x', y')}{\sum_{(x', y' \in c')} f'(x', y')} \right]^p \times \right. \\
 &\quad \left. \left[\frac{\sum_{(x', y' \in c')} y' f'(x', y')}{\sum_{(x', y' \in c')} f'(x', y')} \right]^q \times f(x, y) \right\} \\
 &= \sum_{(x, y \in c)} \left\{ \left[\frac{\sum_{(x, y \in c)} (x + \Delta x) f(x, y)}{\sum_{(x, y \in c)} f(x, y)} \right]^p \times \right. \\
 &\quad \left. \left[\frac{\sum_{(x, y \in c)} (y + \Delta y) f(x, y)}{\sum_{(x, y \in c)} f(x, y)} \right]^q \times f(x, y) \right\} \\
 &= \sum_{(x, y \in c)} \left(x - \frac{\sum_{(x, y \in c)} x f(x, y)}{\sum_{(x, y \in c)} f(x, y)} \right)^p \left(y - \frac{\sum_{(x, y \in c)} y f(x, y)}{\sum_{(x, y \in c)} f(x, y)} \right)^q f(x, y) \\
 &= \sum_{(x, y \in c)} \left(x - \frac{m_{10}}{m_{00}} \right)^p \left(y - \frac{m_{01}}{m_{00}} \right)^q f(x, y) \\
 &= \sum_{(x, y \in c)} (x - \bar{x})^p (y - \bar{y})^q f(x, y) \\
 &= \mu'_{pq} \tag{20}
 \end{aligned}$$

So the seven moments shown in formula (16) are translation invariances according to equations (14) and (15)

2. the rotating invariances of moment feature

Let θ is the variable of rotation for an image, (x, y) and (x', y') is respectively the coordinate of pixels before and after image rotating

$$\begin{cases} x' = x \cos \theta + y \sin \theta \\ y' = y \cos \theta - x \sin \theta \end{cases} \tag{21}$$

That is:

$$\begin{aligned}
 x' - \bar{x}' &= x \cos \theta + y \sin \theta - \frac{m'_{10}}{m'_{00}} \\
 &= x \cos \theta + y \sin \theta - \frac{\sum_{(x,y) \in c} (x \cos \theta + y \sin \theta) f(x,y)}{\sum_{(x,y) \in c} f(x,y)} \quad (2) \\
 &= x \cos \theta + y \sin \theta - \cos \theta \frac{m_{10}}{m_{00}} - \sin \theta \frac{m_{01}}{m_{00}} \\
 &= (x - \bar{x}) \cos \theta + (y - \bar{y}) \sin \theta
 \end{aligned}$$

Similarly, the following formula is attained:

$$y' - \bar{y}' = (y - \bar{y}) \cos \theta - (x - \bar{x}) \sin \theta \quad (23)$$

The relationship of μ'_{20} , μ_{20} and θ can be expressed as following:

$$\begin{aligned}
 \mu'_{20} &= \sum_{(x',y') \in c'} (x' - \bar{x}')^2 f'(x', y') \\
 &= \sum_{(x,y) \in c} [(x - \bar{x}) \cos \theta + (y - \bar{y}) \sin \theta]^2 f(x, y) \quad (24) \\
 &= \sum_{(x,y) \in c} \left[(x - \bar{x})^2 \cos^2 \theta + (y - \bar{y})^2 \sin^2 \theta + \right. \\
 &\quad \left. 2(x - \bar{x})(y - \bar{y}) \sin \theta \cos \theta \right] f(x, y) \\
 &= \mu_{20} \cos^2 \theta + \mu_{02} \sin^2 \theta + 2\mu_{11} \sin \theta \cos \theta
 \end{aligned}$$

Similarly, The relationship among μ'_{02} , μ_{02} and θ is represented as following:

$$\mu'_{02} = \mu_{02} \cos^2 \theta + \mu_{20} \sin^2 \theta - 2\mu_{11} \sin \theta \cos \theta \quad (25)$$

Since

$$\eta'_{20} = \mu'_{20} / \mu_{00}^3 = \mu'_{20} / \mu_{00}^3 \quad (26)$$

$$\eta'_{02} = \mu'_{02} / \mu_{00}^3 = \mu'_{02} / \mu_{00}^3 \quad (27)$$

So

$$\begin{aligned}
 \phi_1 &= \eta'_{20} + \eta'_{02} \\
 &= \frac{(\mu'_{20} + \mu'_{02})}{\mu_{00}^3} \\
 &= \frac{(\mu_{20} \cos^2 \theta + \mu_{02} \sin^2 \theta - 2\mu_{11} \sin \theta \cos \theta + \mu_{02} \cos^2 \theta + \mu_{20} \sin^2 \theta - 2\mu_{11} \sin \theta \cos \theta)}{\mu_{00}^3} \quad (28) \\
 &= \frac{(\mu_{20} + \mu_{02})}{\mu_{00}^3} = \eta_{20} + \eta_{02} = \phi_1
 \end{aligned}$$

From the calculation above, the moment ϕ_1 is proved a rotating invariances for discrete function.

Similarly, the other moments can also be proved the rotating invariances for discrete function.

3. the scale invariances of moment feature

Let ρ is the scale value of an image enlarged or reduced, (x, y) and (x', y') is respectively the coordinate of pixels before and after an image changing (enlarged or reduced) its scale:

$$\begin{cases} x' = \rho x \\ y' = \rho y \end{cases} \quad (29)$$

Then, we can obtain the formula as following:

$$\begin{aligned}
 x' - \bar{x}' &= \rho x - \frac{m'_{10}}{m'_{00}} \\
 &= \rho x - \frac{\sum_{(x,y) \in c} x \rho f(x, y)}{\sum_{(x,y) \in c} \rho f(x, y)} = \rho(x - \bar{x}) \quad (30)
 \end{aligned}$$

Similarly,

$$y' - \bar{y}' = \rho(y - \bar{y}) \quad (31)$$

And further μ'_{pq} can be calculated as following:

$$\begin{aligned}
 \mu'_{pq} &= \sum_{(x',y') \in c'} (x' - \bar{x}')^p (y' - \bar{y}')^q f'(x', y') \\
 &= \sum_{(x,y) \in c} \rho^p (x - \bar{x})^p (y - \bar{y})^q f(x, y) \\
 &= \rho^{p+q} \mu_{pq} \quad (32)
 \end{aligned}$$

Then η'_{pq} is attained:

$$\begin{aligned}
 \eta'_{pq} &= \mu'_{pq} / (\mu_{00}')^{p+q+1} \\
 &= \rho^{p+q} \mu_{pq} / \mu_{00} \\
 &= \rho^{p+q} \eta_{pq} \quad (33)
 \end{aligned}$$

Obviously, there is not the scale invariance of contour moment for discrete function. The moment relates not only with ρ but also with

representation. Given a set of l data vectors $x_i \in R^n$ which are instances of random vector x_i , PCA looks for $m < n$ orthonormal vectors $\{\theta_j\} \in R^n$ which form an orthonormal basis of the subspace that captures maximal variance of the x_i 's. It can be shown that the $\{\theta_j\}$'s are the eigenvectors of the sample covariance matrix Σ of the x_i 's

$$\Sigma = \frac{1}{l} \sum_{i=1}^l (x_i - \bar{x})(x_i - \bar{x})^T \quad (36)$$

Where \bar{x} is the sample mean of the x_i 's. The approximation or reconstruction \hat{x} of the random vector x is the component of x that lies in the subspace expressed in R^m i.e.

$$\hat{x} = \bar{x} + \sum_{j=1}^m (y_j - \bar{y}_j) \theta_j \quad (37)$$

Where $y_i = \theta_i^T x$ is called the i th principal component of x and \bar{y}_i is the i th principal component of the mean \bar{x} , i.e.

$$\bar{y}_i = \theta_i^T \bar{x} \quad (38)$$

By defining the $n \times m$ matrix Φ whose columns are m eigenvectors θ_j of Σ we can write the principal component vector $y \in R^m$

$$y = \Phi^T x \quad (39)$$

and because the columns of Φ are orthonormal, we have

$$\hat{x} = \bar{x} + \Phi(y - \bar{y}) \quad (40)$$

where $\bar{y} = \Phi^T \bar{x}$. A very nice property of PCA is that the mean square error ϵ^2 between x and its reconstruction, which is

$$\epsilon^2 = E[\|x - \hat{x}\|^2],$$

Can be written as

$$\epsilon^2 = \sum_{j=m+1}^n \lambda_j$$

Where λ_j are the eigenvalues of the true covariance matrix generating the x_i 's. This last equation suggests that the mean square error

between x_i and its reconstruction \hat{x} is minimised if the subspace basis contains the m eigenvectors θ_j with the m highest eigenvalues.

The PCA decorrelates the x_i 's as the covariance expressed in the principal subspace

$$\Sigma_y = \Theta^T \Sigma \Theta \quad (41)$$

Is a $m \times m$ diagonal matrix whose diagonal elements are the λ_j 's.

Principal component analysis (PCA) is a useful method for multivariate analysis. The dimensionality of the original features extracted from bacteria images can be reduced using PCA. On knowing the eigenvectors, we can transform the vectors into the eigenbasis. The components of the new vectors are the projections of the old ones onto the eigenvectors. By algebra or a geometry criterion for optimization, We try to describe and to simplify a data matrix of image features, which is represented by some lower dimensional vectors. After analyzing 300 various wastewater images, we estimated the six most relevant eigenvectors which are enough to describe the features of bacteria images for their classification, and the vectors after the sixth component are discarded. Thus the data with 6 dimensions of the features for a type of bacteria image can be attained.

3.4 improved BP Neural Network for Bacteria Recognition.

the ability of an artificial network to learn can be measured by its ability to generalize beyond the examples that it is given during the training procedure. The improved algorithms is proposed to settle the problems in training a BP network:

1. introduce momentum factor in order to accelerate convergence rate and avoid oscillation

$$w(n_0 + 1) = w(n_0) + \eta(n_0) d(n_0) + \alpha \Delta w(n_0)$$

where α is momentum coefficient $0 < \alpha < 1$

Since the direction of correction at time (n_0) depends on the combination correction directions of that both at time $(n_0 - 1)$ and at (n_0) . Furthermore the formula aboved can be transformed as following:

$$w(n_0+1) = w(n_0) + \eta(n_0) \left[d(n_0) + \frac{\alpha}{\eta(n_0)} \right] = w(n_0) + \eta(n_0) \left[d(n_0) + \frac{\alpha \eta(n_0-1)}{\eta(n_0)} d(n_0-1) \right],$$

where $d(n_0)$ and $d(n_0 - 1)$ are not conjugate, so α can moderate the over-correction and under-correction.

2. smooth drive function:

weights modification of both hidden layer and output layer is related to y_s , the output of mid-layer; when y_s is near to 0 or 1 the weights modification approach 0 and the network get into local minimum. For accelerating convergence rate, let $y_s = 0.1$ when $y_s < 0.1$, let $y_s = 0.9$ when $y_s > 0.9$.

3. Adaptive accelerated BP algorithm:

In traditional BP network the lower learning rate usually causes slow convergence rate, while increasing learning rate (η) to accelerate convergence rate can lead to that the convergence rate become instable. So an adaptive adjustment of learning rate is proposed :

$$\omega(k+1) = \omega(k) + \eta(k) D(k)$$

$$\eta(k) = 2^k \eta(k-1)$$

The formula above show that the slow decrease, which is caused by continuous same gradient direction, can be improved by double step length, and the step length is halved for avoiding rapid decrease due to continuous reverse gradient direction. Therefore, the method can keep learning training of the network with proper learning rate.

Four typical kinds of bacteria from CECC database are chosen for training sets, in which the classification is made by the six feature dimensions reduced in 3.2 above. 10 samples for every kind of bacteria are chosen for training set and 6 samples for testing set. The output of the network is 4 types, so the 4-bit binary is used for the classification, that is, 1000 denotes type1, 0100 type2, 0010 type3, type 4 is 0001, and output matrix $T = [1 \ 0 \ 0 \ 0 \ 0 \ 1 \ 0 \ 0 \ 0 \ 0 \ 1 \ 0 \ 0 \ 0 \ 0 \ 1]$. Input neural cell is six and the number of the output is four, moreover, the hidden layer representation function is tansig, which is S type of tangent function. The number of training is 1000, initial learning rate and error is set 0.2 and 2 respectively. The table 4 is shown the comparison of traditional BP algorithm and three kinds of improved BP Neural Network for Bacteria Recognition.

Table 4 Comparison BP and three kinds of improved BP Neural Network for Bacteria Recognition.

Algorithm	Error	Number of Training	time(s)
Traditional BP	2.1362	4200	31.78
Momentum Factor	1.9835	1300	14.54
Smooth Drive Function	1.9924	1000	10.22
Adapt. Accelerated BP	1.9873	745	6.35

The table 4 shows that Adaptive Accelerated BP increases the rapid of training by about 5 times, which is much better than others, so the method is used for Bacteria Recognition. After 387 trainings, the ideal precision is attained within 6.78seconds. 30 images from the database is used to test, and the result shows that the accuracy of recognition rate reach 85.5%.

4 Conclusion

The automatic image analysis procedure is a major step toward completely automatic monitoring of bacterial dynamics in wastewater. It is presented that a novel image of bacteria recognition scheme which is proved effective for identification or determination of bacterial abundance and morphology. A adaptive and enhanced solution is proposed for the edge detection of bacteria images, which intensify the aim object of microscopic image and enhance the clarity of edges. It is performed by optimizing for proper threshold value while exactly locate the aim objects and segment it from background which is achieved by combining the iterative threshold value segmentation theory with mathematical morphology edge detection. The method of edge detection is noise-proof robust, and can be well balanced between refraining noise and the retained whole fine edges of aim

objects. Principal Component Analysis (PCA) is used to reduce the dimensionality of original features extracted from the images and BP network is improved in order to train adaptable for the bacteria images recognition. Experimental results show that the presented image recognition scheme is effective, The proposed method is tested with CECC databases, experimental results demonstrate the presented image recognition scheme is effective, which can greatly improve the speed and consistency in performing large-scale surveys or rapid determination of bacterial abundance, morphology and makes estimation of bacterial condition more accuracy.the speed and consistency in performing large-scale surveys or rapid determination of bacterial abundance, morphology and makes estimation of bacterial condition more accuracy.

Acknowledgment This work was supported by Scientific Research Program of Beijing Municipal Commission of Organization (20081D0501600187) and Research Common Program of China (2005DKA21204-07)

References:

- [1] Gelfand S.B. Mitter S.K. *Netropolis type annealing algorithm for global optimization in Rd*.SIAM J.Control and Optimal 1993(1):70-150.
- [2] J.Liu and T.Zhang., "Fast algorithm for generation of moment invariants ",Pattern Recognition ,vol.33,2004,pp.1745-1756.
- [3] Sungyoung Kim, Sojung Park, and Minhwan Kim, *Image Recognition into Object /Non object Classes*, CIVR 2004, LNCS 3115, pp393-400
- [4] Massana, R., J. M. Gasol, P. K. *Measurements of bacterial size via image analysis of epifluorescence preparations: description of an inexpensive system and solutions to some of the most common problems*. Sci. Mar. 61, 1997, pp397-407.
- [5] Zhang Yujin *Image Engineering(II) Image Analysis* Tsinghua University Press , 2005.
- [6] Drouin, L. Louvel, B. Vanhoutte, *Quantitative characterization of cellular differentiation of Streptomyces ambofaciens in submerged culture by image analysis*, Biotechnology Techniques, 11, 1997,pp819-824 ,
- [7] Cao L J. Chua K S, Chong W K, et al. *A comparison of PCA , KPCA , and ICA for dimensionality reduction in support vector machine [J]*. Neurocomputing, 55 (1- 2) , 2003,pp321 – 336
- [8] R.Mukundan and K.R.Ramakrishnan, *Fast computation of Legendre and Zernike moments*, Pattern Recognition, vol.28,no.9,1995 pp.1433-1442
- [9] J.Flusser, *On the independence of rotation moment invariants*, Pattern Recognition ,vol. 33, no.9, pp.1405-1410
- [10]G.L. Cash and M. Hatamian, "Optical character recognition by the method of moment," Computer Vision,Graphics,and Image Processing, vol. 39,1987,pp.291-310.
- [11]Sieracki, M. E., and C. L. Viles. 1992. *Distributions and fluorochromestaining properties of sub-micrometer particles and bacteria in the North Atlantic*. Deep Sea Res. 39:1919-1929.
- [12]Viles, C. L., and M. E. Sieracki. 1992. *Measurement of marine picoplankton cell size by using a cooled, charge-coupled device camera with image-analyzed fluorescence microscopy*. Appl. Environ. Microbiol. 58:584-592.
- [13] Hu .M.K, *Visual pattern recognition by moment invariant* IEEE Trans .on Information Theory,vol.8,No.2, 1962 ,pp.179-187
- [14] Guoping Qiu, Xia Feng, J ianzhong Fang, *Compressing Histogram Representations for Automatic Colour Photo Categorization*, Pattern Recognition 37, 2004 , pp2177 - 2193
- [15] Li xiaojuan *Local and global features extracting and fusion for microbial recognition* Proceedings - SNPD 2007: Eighth ACIS International Conference on Software Engineering, Artificial Intelligence, Networking, and Parallel/Distributed Computing, 2007, p 507-511
- [16] H. Yu, H. P. Fang, P. J. Yao, Y. Yuan. *A Combined Genetic Algorithm: Simulated Annealing Algorithm for Large Scale System Energy Integration*. Computers and Chemical Engineering, 2000, 24:2023-2035
- [17] Lin Feng-Tse, Kan Cheng-Yon, Hsu Ching-Chi. *Applying the genetic approach to simulated annealing in solving some NP-hard programs*. IEEE Transactions on Systems. Man. And Cybernetics, 1993, 23(6): 1752-1767

- [18] Doloca, Adrian. *Feature Selection for Texture Analysis Using Genetic Algorithm* [J]. *International Journal of Computer Mathematics*, 2000, 74:279~292
- [19] Handels H, Ross T. *Feature Selection for Optimized Skin Tumor Recognition Using Genetic Algorithms* [J]. *Artificial Intelligence in Medicine*, 1999, 16(3):283~297
- [20] Gelfand□S.B. Mitter□S.K. *Netropolis type annealing algorithm for global optimization in Rd*. *SIAM J. Control and Optimal* □ 1993(1):70-150.
- [21] Y. Xu, Y. Zhu and Y. Jia, "Real-time head tracking method," *Journal of Image and Graphics*, vol. 7, no. 1, 2002, pp.11-15.
- [22] S.O. Belkasim and M.Kamel, "Fast computation of 2-D image moments using biaxial transform," *Pattern Recognition*, vol. 34, no. 12, 2001, pp.1867-1877.